Small-Molecule MDM2 Antagonists as a New Therapy Concept for Neuroblastoma

Tom Van Maerken,[1] Frank Speleman,[1] Joëlle Vermeulen,[1] Irina Lambertz,[3] Sarah De Clercq,[3] Els De Smet,[1] Nurten Yigit,[1] Vicky Coppens,[1] Jan Philippé,[2] Anne De Paepe,[1] Jean-Christophe Marine,[3] and Jo Vandesompele[1]

[1]Center for Medical Genetics and [2]Department of Clinical Chemistry, Microbiology, and Immunology, Ghent University Hospital; [3]Laboratory for Molecular Cancer Biology, Flanders Interuniversity Institute for Biotechnology, Ghent, Belgium

Abstract

Circumvention of the p53 tumor suppressor barrier in neuroblastoma is rarely caused by *TP53* mutation but might arise from inappropriately increased activity of its principal negative regulator MDM2. We show here that targeted disruption of the p53-MDM2 interaction by the small-molecule MDM2 antagonist nutlin-3 stabilizes p53 and selectively activates the p53 pathway in neuroblastoma cells with wild-type p53, resulting in a pronounced antiproliferative and cytotoxic effect through induction of G_1 cell cycle arrest and apoptosis. A nutlin-3 response was observed regardless of *MYCN* amplification status. Remarkably, surviving SK-N-SH cells adopted a senescence-like phenotype, whereas CLB-GA and NGP cells underwent neuronal differentiation. p53 dependence of these alternative outcomes of nutlin-3 treatment was evidenced by abrogation of the effects when p53 was knocked down by lentiviral-mediated short hairpin RNA interference. The diversity of cellular responses reveals pleiotropic mechanisms of nutlins to disable neuroblastoma cells and exemplifies the feasibility of exploiting, by a single targeted intervention, the multiplicity of anticancer activities exerted by a key tumor suppressor as p53. The observed treatment effects without the need of imposing a genotoxic burden suggest that selective MDM2 antagonists might be beneficial for treatment of neuroblastoma patients with and without *MYCN* amplification. (Cancer Res 2006; 66(19): 9646-55)

Introduction

As a key cellular gatekeeper, p53 is mutationally inactivated in ~50% of all human malignancies (1, 2). Tumors that retain the wild-type *TP53* gene almost invariably harbor defects in other components of the p53 pathway, either impairing stabilization of p53 in response to stress signals or disrupting essential mediators of p53 transcriptional activity. One such common lesion involves overexpression of the E3 ubiquitin ligase MDM2. This nuclear phosphoprotein is a principal negative regulator of p53 activity and stability by binding to its transactivation domain, promoting its ubiquitination and degradation, favoring its nuclear export, and inhibiting its acetylation (3, 4). As *MDM2* itself is a transcriptional target of p53, it is believed that this system constitutes a negative autoregulatory feedback loop that helps to switch off p53 at the end of a stress response (5, 6). Amplification of *MDM2* or increased expression has been reported in many human neoplasms and has been shown to confer tumorigenic potential (3, 7).

Inhibition of the p53-MDM2 interaction provides an attractive strategy for activating wild-type p53 in tumors and has therefore been the focus of many efforts in anticancer drug discovery. Recently developed potent and selective small-molecule antagonists of MDM2 (8), termed nutlins, bind tightly into the p53 pocket of MDM2, release p53 from negative control, and activate the p53 pathway. This leads to cell cycle arrest and apoptosis in cancer cells with wild-type p53, whereas the response in normal cells, which do not carry the high apoptotic burden characteristic of tumor cells, is limited to a largely reversible growth arrest, except for some bone marrow cell types (8–11). Restoration of p53 function by nutlins may thus have profound therapeutic use for tumors that have retained wild-type p53, particularly if MDM2 activity is inappropriately increased.

Several lines of evidence indicate that nutlins could be effective in the treatment of the neural crest–derived childhood malignancy neuroblastoma. First, <2% of neuroblastoma tumors at diagnosis exhibit mutations in the *TP53* gene, and many studies have revealed an intact p53 pathway in neuroblastoma cells (reviewed in ref. 12). Second, MDM2 is at least in part responsible for the characteristic phenotype of cytoplasmic p53 sequestration in neuroblastoma cells, which may, albeit not precluding p53 activity, limit chemotherapy-induced apoptosis (13). Third, deregulation of MDM2 expression or activity in neuroblastoma has been reported to occur by various means, including amplification of the *MDM2* gene (14–17), loss of production of the MDM2 inhibitory protein $p14^{ARF}$ (17, 18), and transcriptional up-regulation in *MYCN*-amplified neuroblastomas that are associated with poor clinical outcome (19). Finally, inhibition of MDM2 expression or function in neuroblastoma cells results in accumulation of functional p53 in the nucleus (13, 20), further supporting the notion that targeting of MDM2 may offer therapeutic benefit.

These considerations prompted us to investigate the therapeutic potential of disrupting the p53-MDM2 interaction in neuroblastoma. We show that the small-molecule MDM2 antagonist nutlin-3 activates the p53 pathway in neuroblastoma cells with wild-type p53 and elicits a dose- and time-dependent antiproliferative and cytotoxic effect through induction of both G_1 cell cycle arrest and apoptosis regardless of *MYCN* amplification status. Surviving wild-type p53 cells engaged a senescence program in cell line SK-N-SH or a neuronal differentiation process in cell lines CLB-GA and NGP, which were prevented by lentiviral-mediated expression of p53 short hairpin RNA (shRNA). The pronounced effects of nutlin-3 on

Note: Supplementary data for this article are available at Cancer Research Online (http://cancerres.aacrjournals.org/).

This article presents research results of the Belgian program of Interuniversity Poles of Attraction initiated by the Belgian State, Prime Minister's Office, Science Policy Programming.

Requests for reprints: Tom Van Maerken, Center for Medical Genetics, Ghent University Hospital, De Pintelaan 185, B-9000 Ghent, Belgium. Phone: 32-9-240-39-46; Fax: 32-9-240-65-49; E-mail: tom.vanmaerken@UGent.be.

doi:10.1158/0008-5472.CAN-06-0792

neuroblastoma cells and the identification of premature senescence and differentiation as drug-induced response programs, not yet described for selective MDM2 antagonists but of potential clinical importance, may provide a novel therapy concept for neuroblastoma patients with and without *MYCN* amplification.

Materials and Methods

Cell lines and nutlin-3 treatment. Nine human neuroblastoma cell lines were used for this study: CLB-GA, IMR-32, LA-N-5, LA-N-6, NBL-S, NGP, SK-N-BE(2c), SK-N-FI, and SK-N-SH. Cell lines were grown as monolayers in RPMI 1640 supplemented with antibiotics, 15% FCS, and 2 mmol/L glutamine at 37°C and 5% CO_2 in a humidified atmosphere. Nutlin-3 (Cayman Chemical, Ann Arbor, MI) was dissolved in ethanol and stored as a 10 mmol/L stock solution in small aliquots at −20°C. Cells were exposed to 0 to 32 μmol/L nutlin-3 for the time period indicated, with the final ethanol concentration kept constant in each experiment. Cellular morphology was examined under an inverted (phase contrast) microscope, and images were taken using Canon PowerShot S45 digital camera (Canon, Tokyo, Japan) and Remote Capture software version 2.6.0.

Gene copy number determination of *MYCN* and *MDM2*. Copy numbers for *MYCN* and *MDM2* were determined using a real-time quantitative PCR assay with SYBR Green I detection chemistry as described previously (21). Two reference genes, *TNFRSF17* (*BCMA*) and *SDC4*, were used for normalization. Primer sequences are available in the public RTPrimerDB database[4] (22): *TNFRSF17* (14), *SDC4* (15), *MYCN* (11), and *MDM2* (3498).

Real-time quantitative reverse transcription-PCR–based quantification of mRNA expression. Total RNA extraction from cells treated with 0, 2, 4, 8, 16, and 32 μmol/L nutlin-3 for 24 hours (all cell lines) and from cells treated with 0 and 16 μmol/L nutlin-3 for 1, 2, 3, and 7 days (NGP and CLB-GA cells), DNase treatment, cDNA synthesis, and SYBR Green I reverse transcription-PCR (RT-PCR) were carried out as described (23, 24). Primer sequences are available in RTPrimerDB[4] (22): *GAPDH* (3), *SDHA* (7), *UBC* (8), *MDM2* (3499), *CDKN1A* (*p21*$^{WAF1/CIP1}$; 631), *BAX* (814), *BBC3* (*PUMA*; 3500), *TP53I3* (*PIG3*; 3501), *ASCL1* (*HASH1*; 373), *CHAT* (3502), *CHGA* (474), *CHGB* (3503), *DBH* (1086), *DDC* (365), *ENO2* (3506), *GAP43* (97), *HAND2* (98), *HNT* (1078), *IGF2* (103), *NEFH* (3504), *NEFL* (3505), *NEF3* (*NEFM*; 3507), *NPY* (117), *NTRK1* (*TRKA*; 118), *NTRK2* (*TRKB*; 119), *PNMT* (1087), *PRPH* (3508), *STMN2* (129), *TH* (3510), *TTBK2* (3509), and *TUBB3* (3511). Gene expression levels were determined using our in-house developed qBase analysis software[5,6] using a δ-C_t relative quantification model with PCR efficiency correction and multiple reference gene normalization (*GAPDH, UBC*, and *SDHA*; ref. 24).

***TP53* mutation analysis.** Total RNA extraction from untreated cells, DNase treatment, and cDNA synthesis were done as detailed above. The entire coding region of *TP53* was PCR amplified in two overlapping fragments using the following primer pairs: 5′-GTGACACGCTTCCCTGGATT-3′ (forward) and 5′-GCACCACCACACTATGTCGAA-3′ (reverse) and 5′-GCGTCCGCGCCATG-3′ (forward) and 5′-GCAAGCAAGGGTTCAAAGACC-3′ (reverse). After purification with exonuclease I (New England Biolabs, Ipswich, MA) and antarctic phosphatase (New England Biolabs), PCR products were sequenced using the BigDye Terminator v3.1 Cycle Sequencing kit (Applied Biosystems, Foster City, CA) and the same primers as those used in the PCR. Sequencing reactions were cleaned up with the CleanSEQ magnetic bead system (Agencourt, Beverly, MA), loaded onto an ABI3730 XL DNA sequencer (Applied Biosystems), and analyzed with SeqScape software version 2.5 (Applied Biosystems).

Western blot analysis. Cells treated with 0 or 16 μmol/L nutlin-3 for 24 hours were solubilized in lysis buffer containing 1% Triton X-100, 150 mmol/L NaCl, 50 mmol/L HEPES (pH 7.5), 1 mmol/L EDTA, 2.5 mmol/L EGTA, 1 mmol/L NaF, 10 mmol/L β-glyceralphosphate, and protease and phosphatase inhibitor cocktails (Sigma, St. Louis, MO). Cell lysates were sonicated and centrifuged for 2 minutes at 12,000 rpm. Total protein (60 μg) was fractionated on 12% SDS polyacrylamide gel, transferred to a Hybond-P membrane (Amersham Biosciences, Piscataway, NJ), and probed with antibodies against total p53 (Santa Cruz Biotechnology, Santa Cruz, CA), MDM2 (Santa Cruz Biotechnology), p21$^{WAF1/CIP1}$ (Santa Cruz Biotechnology), and BAX (Upstate, Charlottesville, VA). The membrane was probed for γ-tubulin (Sigma) as loading control after being stripped with 62.5 mmol/L Tris, 2% SDS, and 100 mmol/L β-mercaptoethanol for 30 minutes at 50°C. Secondary antibodies were anti-rabbit horseradish peroxidase (HRP; Amersham Biosciences), anti-mouse HRP (Amersham Biosciences), and anti-goat HRP (Abcam, Cambridge, United Kingdom). Proteins were visualized using enhanced chemiluminescence detection reagents (Amersham Biosciences) and exposure to an LS imaging film (Kodak, Rochester, NY).

Cell viability assay. Cells were seeded in duplicate in 96-well plates (10^4 per well), incubated for 6 hours to permit adherence to the surface, and then treated with 0 to 32 μmol/L nutlin-3 for 12, 24, 48, and 72 hours. Cell viability was determined using the CellTiter-Glo Luminescent Cell Viability Assay (Promega, Madison, WI). Three independent experiments were done.

Cell cycle analysis. For analysis of cell cycle distribution, 10^6 CLB-GA, IMR-32, NGP, SK-N-BE(2c), and SK-N-SH cells were cultured in the presence of 16 μmol/L nutlin-3 or an equivalent amount of ethanol for 24 and 48 hours, trypsinized, washed with PBS, and incubated for 15 minutes with propidium iodide to stain DNA. Cellular DNA content was analyzed in an FC500 flow cytometer (Beckman Coulter, Miami, FL). Cell cycle fractions were quantified using WinCycle software (Phoenix Flow Systems, San Diego, CA).

DNA fragmentation assay. DNA from LA-N-5, SK-N-SH, and SK-N-BE(2c) cells treated with 0 or 16 μmol/L nutlin-3 for 24 hours was extracted using the Suicide Track DNA Ladder Isolation kit (Calbiochem, San Diego, CA), analyzed on a 1.5% agarose gel containing ethidium bromide, and visualized by UV light. A positive DNA ladder control (HL60 cells treated with 0.5 μg/mL actinomycin D for 19 hours) was supplied with the kit.

Analysis of caspase-3 and caspase-7 activity. Cells were plated in duplicate in 96-well plates (5×10^3 per well), incubated for 6 hours, and then treated with 0 to 32 μmol/L nutlin-3 for 12 and 24 hours. The combined activity of caspase-3 and caspase-7 was determined using the Caspase-Glo 3/7 Assay (Promega) and corrected for cell viability. Each condition was tested in three independent experiments.

Cellular senescence assay. For senescence-associated β-galactosidase (SA-β-gal) staining, 2.5×10^5 cells were seeded in 35-mm dishes, grown for 24 hours, and then exposed to 16 μmol/L nutlin-3 or to an equivalent amount of ethanol for 1 and 7 days. Control cultures for 7 days were split every 3 days to avoid confluency. Fixation of cells and staining for SA-β-gal activity at pH 6.0 were done with the Senescent Cells Staining kit (Sigma). SA-β-gal activity was scored in 1,800 to 2,000 cells from three microscopy fields.

Lentiviral vector construction, virus production, and infection. The sequence of the human *TP53* gene chosen to be shRNA targeted was 5′-GACTCCAGTGGTAATCTAC-3′. As a negative control, we used a shRNA specific for the mouse form of p53 (*Trp53*): 5′-GTACTCTCCTCCCCTCAAT-3′. Additional control shRNA constructs for SK-N-SH cells were directed against a different region of the murine *Trp53* gene (5′-GTACATGTGTAATAGCTCC-3′) and against firefly luciferase (5′-GTGCGTTGTTAGTACTAATCCTATTT-3′). Pairs of complementary oligonucleotides containing these sequences were phosphorylated, annealed, and ligated into the pSIF-H1-Puro vector (System Biosciences, Mountain View, CA).

Human embryonic kidney 293T cells were cultured at 37°C and 5% CO_2 in DMEM supplemented with antibiotics, 10% FCS, and 2 mmol/L glutamine. Transfections of 293T cells were done with the calcium phosphate precipitation technique. The pSIF-H1-Puro vectors containing the shRNA sequences were cotransfected with two packaging plasmids: pFIV-34N and pVSV-G (System Biosciences). Viral supernatants were collected and

[4] http://medgen.ugent.be/rtprimerdb.
[5] http://medgen.ugent.be/qbase.
[6] J. Hellemans, G. Mortier, A. De Paepe, F. Speleman, and J. Vandesompele. qBase relative quantification framework and software for management and automated analysis of real-time quantitative PCR data, in preparation.

filtered through a 0.45-μm filter. NGP and SK-N-SH cells were infected with lentiviruses carrying the shRNA constructs described above in the presence of 5 μg/mL polybrene (Sigma). Transduced cells were selected with 1 μg/mL puromycin (Sigma) for 48 hours.

Results

Genetic characterization of neuroblastoma cell lines and effect of nutlin-3 on cell viability. All nine cell lines used in this study were characterized with respect to the current *TP53* mutational status and the gene copy number of *MDM2* and *MYCN* (Table 1). cDNA sequence analysis of the entire coding region revealed wild-type *TP53* in CLB-GA, IMR-32, LA-N-5, LA-N-6, NBL-S, NGP, and SK-N-SH cells. Cell line SK-N-BE(2c) carried a 404G>T (C135F) missense mutation in *TP53* as previously reported (25). In SK-N-FI cells, we found a 737T>G (M246R) missense *TP53* mutation, which has been described in other malignancies originating from the breast, colorectum, esophagus, liver, and skin (2). Gene copy number determination using a real-time quantitative PCR assay showed *MDM2* amplification in one cell line, NGP, and *MYCN* amplification in cell lines IMR-32, LA-N-5, NGP, and SK-N-BE(2c).

To address if inhibition of the p53-MDM2 interaction might offer therapeutic potential for neuroblastoma, we examined the antiproliferative and cytotoxic effect of nutlin-3 on this panel of cell lines (Fig. 1; Supplementary Fig. S1). In keeping with the normal *TP53* status, a pronounced dose- and time-dependent decrease in cell viability on nutlin-3 treatment was recorded for cell lines LA-N-5, NBL-S, IMR-32, NGP, SK-N-SH, and CLB-GA (reduction in cell viability after 72 hours of incubation with 32 μmol/L nutlin-3: 100%, 98%, 98%, 96%, 95%, and 86%, respectively). LA-N-6 cells, which also carry wild-type *TP53*, displayed a more moderate decrease in cell viability throughout the whole range of tested nutlin-3 concentrations. The two cell lines with *TP53* mutation, SK-N-BE(2c) and SK-N-FI, did not respond to low nutlin-3 concentrations but nonetheless exhibited a similar cell viability reduction as LA-N-6 cells at the highest tested concentration of 32 μmol/L.

We next looked at the possibility that amplification of *MDM2* or *MYCN*, the latter being reported to exert its oncogenic activity partly through direct transcriptional up-regulation of *MDM2* (19), influences the cell viability response to nutlin-3. No difference in nutlin-3-induced cell viability reduction was observed with respect to *MDM2* or *MYCN* amplification status ($P > 0.05$, Mann-Whitney U test). Although for *MDM2* this result should be interpreted with some caution because only one cell line displayed *MDM2* amplification, the equal distribution of the four *MYCN*-amplified and the five *MYCN*-nonamplified cell lines in relation to cell viability response indicates that *MYCN* amplification does not enhance the antiproliferative and cytotoxic activity of nutlin-3.

Table 1. *TP53* mutational status, *MDM2* copy number status, and *MYCN* copy number status of neuroblastoma cell lines studied

Cell line	*TP53**	*MDM2*†	*MYCN*†
CLB-GA	wt	N	N
IMR-32	wt	N	amp
LA-N-5	wt	N	amp
LA-N-6	wt	N	N
NBL-S	wt	N	N
NGP	wt	amp	amp
SK-N-BE(2c)	404G>T (C135F)	N	amp
SK-N-FI	737T>G (M246R)	N	N
SK-N-SH	wt	N	N

Abbreviations: wt, wild-type; amp, amplified; N, nonamplified.
*From direct DNA sequencing of the entire coding region of *TP53*. Mutation is indicated by nucleotide change followed by amino acid change.
†Genomic amplification status.

Nutlin-3 induces expression of p53 target genes, cell cycle arrest, and apoptosis in neuroblastoma cells with wild-type p53. According to the proposed mechanism of action, the reduction in cell viability after nutlin-3 treatment should result from activation of the p53 pathway, leading to cell cycle arrest and apoptosis. In keeping with this assumption, exposure of cells with wild-type p53 to nutlin-3 for 24 hours induced an increase in mRNA levels of p53 target genes involved in autoregulation (*MDM2*), cell cycle arrest [*CDKN1A* (*$p21^{WAF1/CIP1}$*)], and apoptosis [*BAX, BBC3* (*PUMA*), and *TP53I3* (*PIG3*)] in a dose-dependent manner, as is shown in Fig. 2*A* for CLB-GA, IMR-32, NGP, and SK-N-SH cells. In contrast, expression of p53 target genes was not influenced by nutlin-3 treatment in SK-N-BE(2c) cells carrying a *TP53* mutation (Fig. 2*A*). Western blot analysis at the selected concentration of 16 μmol/L nutlin-3 confirmed stabilization of p53 protein and up-regulation of MDM2, $p21^{WAF1/CIP1}$, and BAX expression in neuroblastoma cells with wild-type p53 (Fig. 2*B*). SK-N-BE(2c) cells with *TP53* mutation exhibited a moderate accumulation of p53 protein on nutlin-3 treatment, compatible with the release from MDM2-mediated degradation, without induction of expression of p53 target genes (Fig. 2*B*). Similar results were observed at both mRNA and protein level for all other neuroblastoma cell lines in this study (Supplementary Figs. S2 and S3).

Flow cytometric cell cycle profiling of CLB-GA, IMR-32, NGP, and SK-N-SH cells at 24 and 48 hours revealed that 16 μmol/L nutlin-3 induced accumulation of cells with wild-type p53 in G_1 phase and a decrease in the percentage of cells in S phase (Fig. 3*A*). Inhibition of the G_1-S transition after exposure to nutlin-3 was absent in the p53 mutant cell line SK-N-BE(2c) (Fig. 3*A*). Treatment of wild-type p53 cells with nutlin-3 induced apoptosis as evidenced by increased sub-G_1 DNA content (Fig. 3*A*), DNA laddering fragmentation on agarose gel electrophoresis (Fig. 3*B*), and activation of caspase-3 and caspase-7 in a dose- and time-dependent fashion (Fig. 3*C*). Control experiments with p53 mutant SK-N-BE(2c) cells revealed no apoptotic features up to a concentration of 16 μmol/L nutlin-3, but an appreciable increase in caspase-3 and caspase-7 activity was observed after treatment with 32 μmol/L nutlin-3 (Fig. 3*A-C*).

Taken together, these data indicate that nutlin-3 activates the p53 pathway selectively in neuroblastoma cells with wild-type p53 and exerts a dose- and time-dependent antiproliferative and cytotoxic effect through induction of both G_1 cell cycle arrest and apoptosis.

Induction of premature cellular senescence in the surviving fraction of SK-N-SH cells by nutlin-3. The therapeutic effect of most conventional anticancer drugs has been attributed for years to their ability to induce apoptotic cell death. More recently, it has been recognized that a terminal growth arrest with morphologic and expression features reminiscent of replicative senescence, termed premature or accelerated cellular senescence, constitutes an alternative drug-induced response program controlled by p53 and $p16^{INK4a}$ (26). Therefore, we next addressed the question of

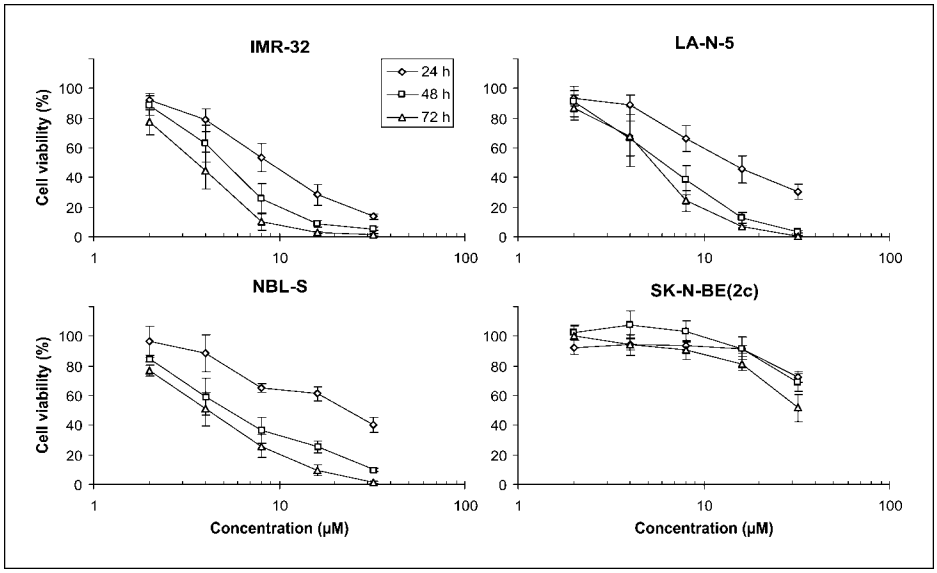

Figure 1. Effect of nutlin-3 on cell viability of neuroblastoma cell lines. Exponentially growing neuroblastoma cells with wild-type p53 (IMR-32, LA-N-5, and NBL-S) or *TP53* mutation [SK-N-BE(2c)] were exposed to a range of nutlin-3 concentrations for 24, 48, and 72 hours, and the percentage cell viability with respect to controls was determined. *Points,* average of three different experiments, each done in duplicate; *bars,* SD. Cell viability results for the complete panel of neuroblastoma cell lines studied are available as Supplementary Data, Fig. S1.

whether targeted disruption of the p53-MDM2 interaction could trigger a premature senescence response in cells surviving nutlin-3 treatment.

Striking morphologic alterations characteristic of senescent cells were indeed observed in SK-N-SH cells on nutlin-3 administration, including a flattened and enlarged cell shape with increased cytoplasmic granularity (Fig. 4*A*). Gene expression of the cell cycle inhibitor *CDKN1A* was increased 14-fold after 24 hours of incubation with 16 μmol/L nutlin-3 (Fig. 2*A*), with ~70% of cells residing in G_1 phase (Fig. 3*A*). SA-β-gal activity was examined to further define the phenotypic changes in SK-N-SH cells surviving nutlin-3 exposure. Approximately 2.5×10^5 SK-N-SH cells were seeded into 35-mm dishes, cultured for 24 hours, and then treated with 16 μmol/L nutlin-3 or vehicle control. Staining for SA-β-gal activity after 24 hours of treatment revealed that control cultures contained low numbers of SA-β-gal-expressing cells [45 per mm^2 cell culture area; 95% confidence interval (95% CI), 32-58; Fig. 4*A*]. Treatment with 16 μmol/L nutlin-3 significantly enhanced the number of SA-β-gal-expressing cells with rapid kinetics (411 per mm^2 after 24 hours; 95% CI, 371-451; $P < 0.0001$), suggesting that nutlin-3 does not just select for SA-β-gal-expressing cells but actively induces a senescence-like phenomenon in surviving SK-N-SH cells. After 7 days of exposure to 16 μmol/L nutlin-3, ~100% of SK-N-SH cells not subject to apoptotic cell death stained positive for SA-β-gal and had acquired a senescence-like morphology (Fig. 4*A*).

SA-β-gal analysis of all other neuroblastoma cell lines with a fraction of cells surviving nutlin-3 treatment [CLB-GA, LA-N-6, and NGP cells, all with wild-type p53, and SK-N-BE(2c) and SK-N-FI cells harboring a *TP53* mutation] revealed that progressive SA-β-gal accumulation during nutlin-3 treatment also occurred in NGP and CLB-GA cells (data not shown). SA-β-gal staining intensity was however considerably weaker than in SK-N-SH cells, and morphologic signs of cellular senescence were absent in these two cell lines, suggesting that the increase in SA-β-gal activity did not concern a genuine senescence response.

Induction of sympathetic neuronal differentiation in the surviving fraction of NGP and CLB-GA cells by nutlin-3. The morphologic changes induced by nutlin-3 in surviving NGP and CLB-GA cells were markedly different from those in SK-N-SH cells. As shown in Fig. 4*B*, addition of nutlin-3 to NGP and CLB-GA cultures provoked hallmarks of neuronal differentiation in cells surviving the treatment, such as the acquisition of a bipolar or multipolar cell shape, the development and extensive outgrowth of neurites with varicosities and growth cone-like endings, and the formation of netlike arrangements of neuronal processes.

Phenotypic characterization of the differentiation process was done by assessing mRNA expression levels of 23 neuronal or neuroendocrine differentiation marker genes at 1, 2, 3, and 7 days of treatment with 16 μmol/L nutlin-3. Selected results for NGP cells are shown in Fig. 4*C* (all results available in Supplementary Fig. S4). The neurite outgrowth in nutlin-3-treated NGP cells was confirmed by increased expression of genes encoding neurofilament constituents (*NEFL, NEF3*, and *NEFH*), a gene encoding an axonal protein with an established role in growth cone and synapse formation (*GAP43*), and a gene reported to promote neurite outgrowth and adhesion (*HNT*). Expression of several marker genes typically associated with neuroendocrine chromaffin differentiation in the developing sympathetic nervous system (27, 28) did not change (*CHGB* and *TH*), decreased (*CHGA*), or increased (*IGF2*) on nutlin-3 treatment of NGP cells, the latter possibly related to a role of IGF2 as an autocrine and paracrine survival factor in a negative autoregulatory feedback fashion (29). As for *TH*, no significant increase in mRNA levels of other genes involved in catecholamine biosynthesis (*DDC, DBH*, and *PNMT*) was detected, but expression of the neuropeptide *NPY*, which in the developing sympathetic nervous system is confined to the neuronal lineage (27), was significantly up-regulated. The most dramatic gene expression change in nutlin-3-treated NGP cells consisted of an ~500-fold increase in expression of the gene responsible for acetylcholine biosynthesis (*CHAT*), indicative of differentiation along a cholinergic neuronal lineage. Interestingly, nutlin-3 treatment of NGP cells also induced a shift in the neurotrophin receptor expression profile toward up-regulation of *NTRK1* (*TRKA*) and suppression of *NTRK2* (*TRKB*) expression, consistent with the acquisition of a less aggressive phenotype (reviewed in ref. 30).

Neuronal/neuroendocrine marker expression analysis of CLB-GA cells after nutlin-3 treatment also confirmed the process of neuronal differentiation as evidenced by elevated expression of several genes involved in neurite outgrowth (*NEFL, PRPH*, and

HNT; Fig. 4*D*). For this cell line, however, we observed a marked down-regulation of *CHAT* expression along with a transient up-regulation of expression of several catecholaminergic genes (*TH* and *DBH*), sympathetic neuroendocrine markers (*CHGA, CHGB, IGF2*, and *TH*), and the sympathetic neuronal marker *NPY* (Supplementary Fig. S5). This transient coexpression of sympathetic neuronal and neuroendocrine markers mimics the maturation process in some neuroblastoma tumors (27) and might reflect the multipotent differentiation capacity of immature neuroblasts before a definite commitment is made. A nutlin-3-induced shift toward a more favorable neurotrophic tyrosine kinase receptor pattern was again observed, resulting from a >100-fold reduction of *NTRK2* expression together with a transient increase in *NTRK1* expression (Fig. 4*D*).

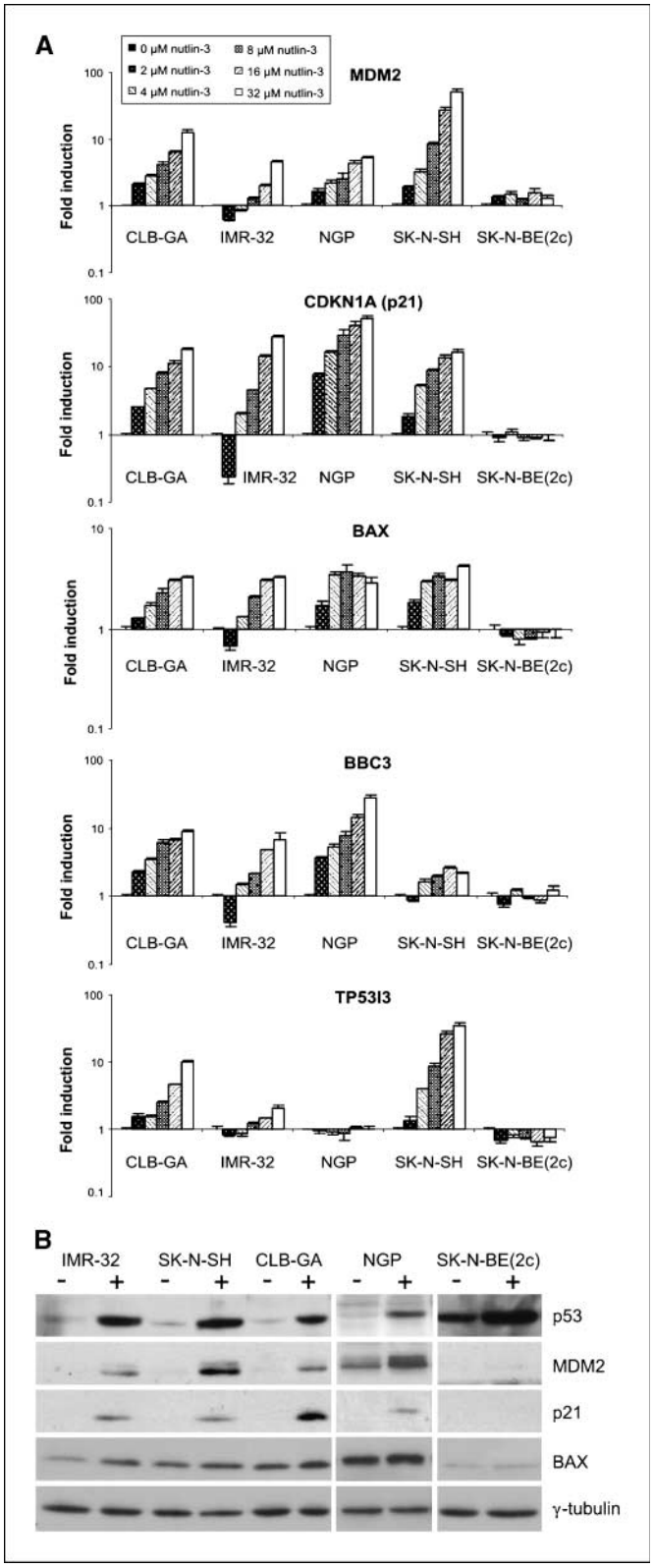

Figure 2. Nutlin-3 treatment stabilizes p53 and selectively induces expression of p53 target genes in neuroblastoma cells with wild-type p53. *A,* CLB-GA, IMR-32, NGP, and SK-N-SH cells with wild-type p53 and SK-N-BE(2c) cells with *TP53* mutation were treated with 0 to 32 μmol/L nutlin-3 for 24 hours, and expression of p53 target genes with a role in autoregulation (*MDM2*), cell cycle arrest [*CDKN1A* (*p21*$^{WAF1/CIP1}$)], and apoptosis [*BAX, BBC3* (*PUMA*), and *TP53I3* (*PIG3*)] was analyzed by real-time quantitative RT-PCR. Results are fold induction of mRNA expression compared with vehicle-treated cells. The lack of up-regulation of *TP53I3* expression in NGP cells was unexpected and suggests that PIG3 is nonfunctional in this cell line. *Columns,* mean of two different RT-PCR measurements; *bars,* SE. *B,* Western blot analysis of p53, MDM2, p21$^{WAF1/CIP1}$, and BAX expression in neuroblastoma cells with wild-type p53 (IMR-32, SK-N-SH, CLB-GA, and NGP) or with *TP53* mutation [SK-N-BE(2c)] after treatment with 16 μmol/L nutlin-3 (+) or an equivalent amount of solvent (−) for 24 hours. Expression of γ-tubulin for each lysate as a loading control. Results of nutlin-3-induced changes in mRNA and protein expression levels of p53 target genes for all cell lines in this study are available as Supplementary Data, Figs. S2 and S3.

Induction of premature senescence in SK-N-SH cells and neuronal differentiation in NGP cells by nutlin-3 is p53 dependent. To evaluate whether the premature senescence response in SK-N-SH cells and the neuronal differentiation in NGP cells are a direct consequence of nutlin-3-induced activation of wild-type p53, we infected SK-N-SH and NGP cells with a lentiviral vector encoding a shRNA directed specifically against human p53 (LV-h-p53) or murine p53 (LV-m-p53). Knockdown of human p53 severely attenuated the cell viability reduction after nutlin-3 treatment in both SK-N-SH and NGP cells (Fig. 5*A*). In contrast, control infection with LV-m-p53 did not affect the nutlin-3 response in NGP cells, but unexpectedly, we observed some attenuation of response in SK-N-SH cells infected with LV-m-p53 (Fig. 5*A*). Control infection of SK-N-SH cells was therefore repeated using the same LV-m-p53 vector, a lentiviral vector encoding a shRNA against a different target site in the murine *Trp53* gene (LV-m2-p53), and a lentiviral vector carrying a shRNA construct specific for firefly luciferase (LV-luc). This yielded in all cases a distinct dose- and time-dependent cell viability response to nutlin-3, similar to the example shown in Fig. 5*A* and indicative of p53 functionality. Western blot analysis of p53 and p21$^{WAF1/CIP1}$ expression showed induction of a p53 response after treatment with 16 μmol/L nutlin-3 for 24 hours in all three types of control-infected SK-N-SH cells but not in LV-h-p53-infected SK-N-SH cells (Fig. 5*B*), validating selective impairment of p53 function in the latter cells.

Transduction of SK-N-SH cells with LV-h-p53 prevented nutlin-3-induced premature senescence as evidenced by cell morphology evaluation and staining for SA-β-gal activity (Fig. 5*C*). Incubation of LV-h-p53-infected SK-N-SH cells with 16 μmol/L nutlin-3 for 24 hours did not induce phenotypic alterations and yielded a similar low density of SA-β-gal-expressing cells (53 per mm^2 cell culture area; 95% CI, 39-67) as treatment of a parallel culture, plated at the same initial cell density, with vehicle control for 24 hours (58 per mm^2; 95% CI, 43-73; $P > 0.05$). Induction of neuronal differentiation by nutlin-3 in NGP cells was also completely abolished when human p53 was silenced. Cultures of NGP cells

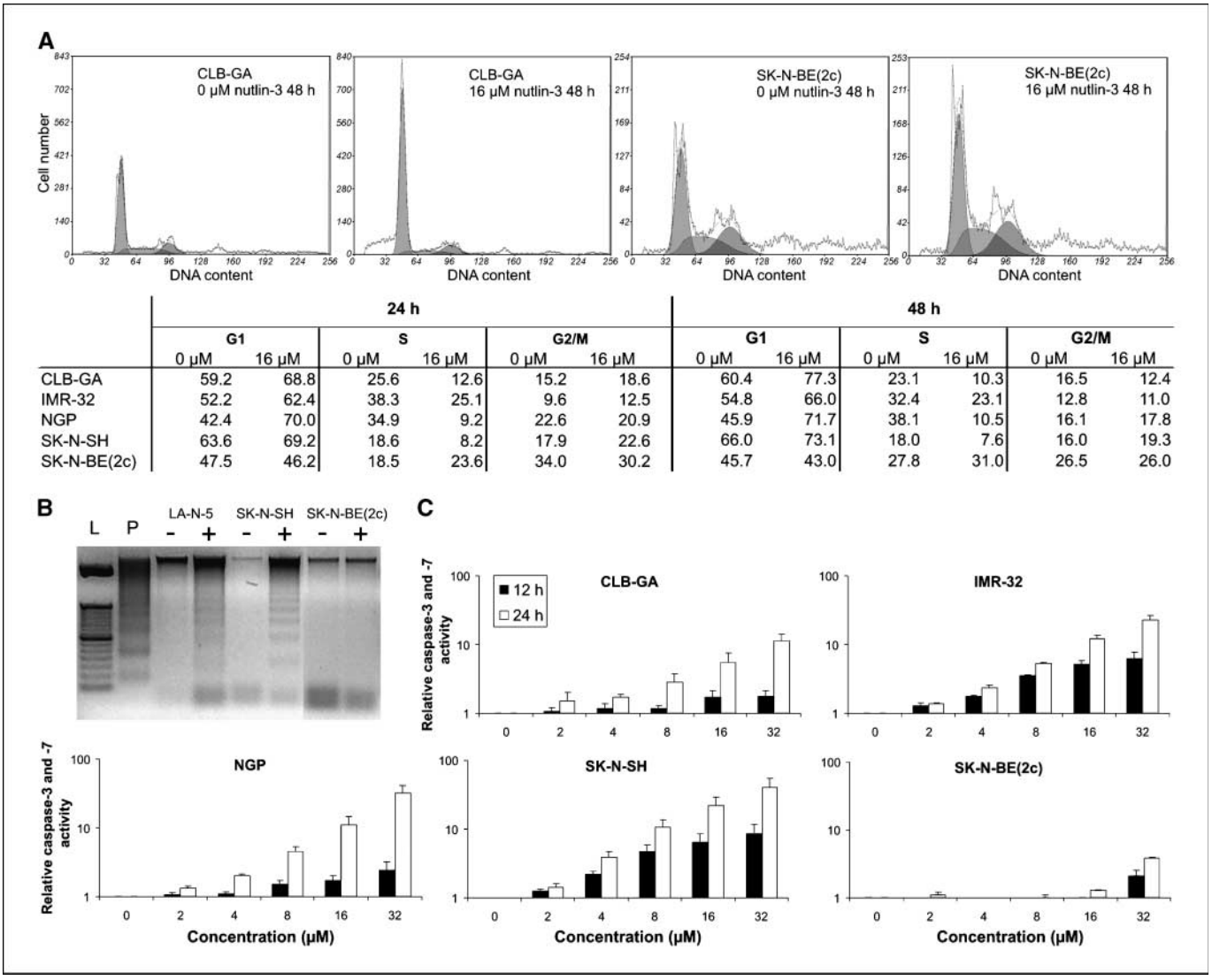

	24 h						48 h					
	G1		S		G2/M		G1		S		G2/M	
	0 μM	16 μM	0 μM	16 μM	0 μM	16 μM	0 μM	16 μM	0 μM	16 μM	0 μM	16 μM
CLB-GA	59.2	68.8	25.6	12.6	15.2	18.6	60.4	77.3	23.1	10.3	16.5	12.4
IMR-32	52.2	62.4	38.3	25.1	9.6	12.5	54.8	66.0	32.4	23.1	12.8	11.0
NGP	42.4	70.0	34.9	9.2	22.6	20.9	45.9	71.7	38.1	10.5	16.1	17.8
SK-N-SH	63.6	69.2	18.6	8.2	17.9	22.6	66.0	73.1	18.0	7.6	16.0	19.3
SK-N-BE(2c)	47.5	46.2	18.5	23.6	34.0	30.2	45.7	43.0	27.8	31.0	26.5	26.0

Figure 3. Inhibition of the G_1-S transition and induction of apoptosis by nutlin-3 in neuroblastoma cells with wild-type p53. *A,* CLB-GA, IMR-32, NGP, and SK-N-SH cells with wild-type p53 and SK-N-BE(2c) cells with *TP53* mutation were incubated with 0 or 16 μmol/L nutlin-3 for 24 and 48 hours, and cell cycle distribution was monitored by flow cytometry. DNA content histograms of CLB-GA and SK-N-BE(2c) cells after 48 hours of treatment (*top*) together with the percentage of cells in G_1, S, and G_2/M phases after 24 and 48 hours for all cell lines (*bottom*). *B,* agarose gel electrophoresis of DNA extracted from neuroblastoma cells with wild-type p53 (LA-N-5 and SK-N-SH) or with *TP53* mutation [SK-N-BE(2c)] following incubation with 0 μmol/L (−) or 16 μmol/L (+) nutlin-3 for 24 hours. Exposure of LA-N-5 and SK-N-SH cells to nutlin-3 resulted in the appearance of a DNA laddering pattern characteristic of apoptosis, whereas no DNA fragmentation was observed after treatment of SK-N-BE(2c) cells with 16 μmol/L nutlin-3. *L,* 50 bp ladder; *P,* positive DNA ladder control. *C,* combined caspase-3 and caspase-7 activity in CLB-GA, IMR-32, NGP, and SK-N-SH cells with wild-type p53 and in SK-N-BE(2c) cells with *TP53* mutation on treatment with a range of nutlin-3 concentrations for 12 and 24 hours relative to a similar amount of viable control cells. *Columns,* average of three different experiments, each done in duplicate; *bars,* SD.

infected with LV-h-p53 did not exhibit morphologic changes when treated with 16 μmol/L nutlin-3 for 7 days (Fig. 5*C*), which was confirmed by the absence of consistent changes in the mRNA expression pattern of neuronal/neuroendocrine marker genes after 7 days of treatment with 16 μmol/L nutlin-3 compared with vehicle control (Fig. 5*D*). These results indicate that nutlin-3 induces premature senescence in SK-N-SH cells and neuronal differentiation in NGP cells in a p53-dependent manner, consistent with targeted inhibition of the p53-MDM2 interaction.

Discussion

Neuroblastoma accounts for ~15% of all childhood cancer deaths (31) and often confronts survivors later in life with severe genotoxic side effects of treatment. Direct and specific activation of the p53 pathway without inducing collateral DNA damage offers a tantalizing answer to the shortcomings of current therapeutic regimens and seems a reasonable approach for neuroblastoma in view of the infrequent occurrence of *TP53* mutations. Cumulative evidence of inappropriately increased MDM2 activity in neuroblastoma incited us to examine the effects of targeted inhibition of the p53-MDM2 interaction by nutlin-3 in neuroblastoma cells. We found that treatment with nutlin-3 stabilizes p53 and selectively induces expression of p53 target genes in neuroblastoma cells with wild-type p53, leading to G_1 cell cycle arrest and apoptosis. Of particular interest is the observation of alternative nutlin-3 response programs in surviving cells (i.e., premature cellular senescence in SK-N-SH cells and neuronal differentiation in NGP

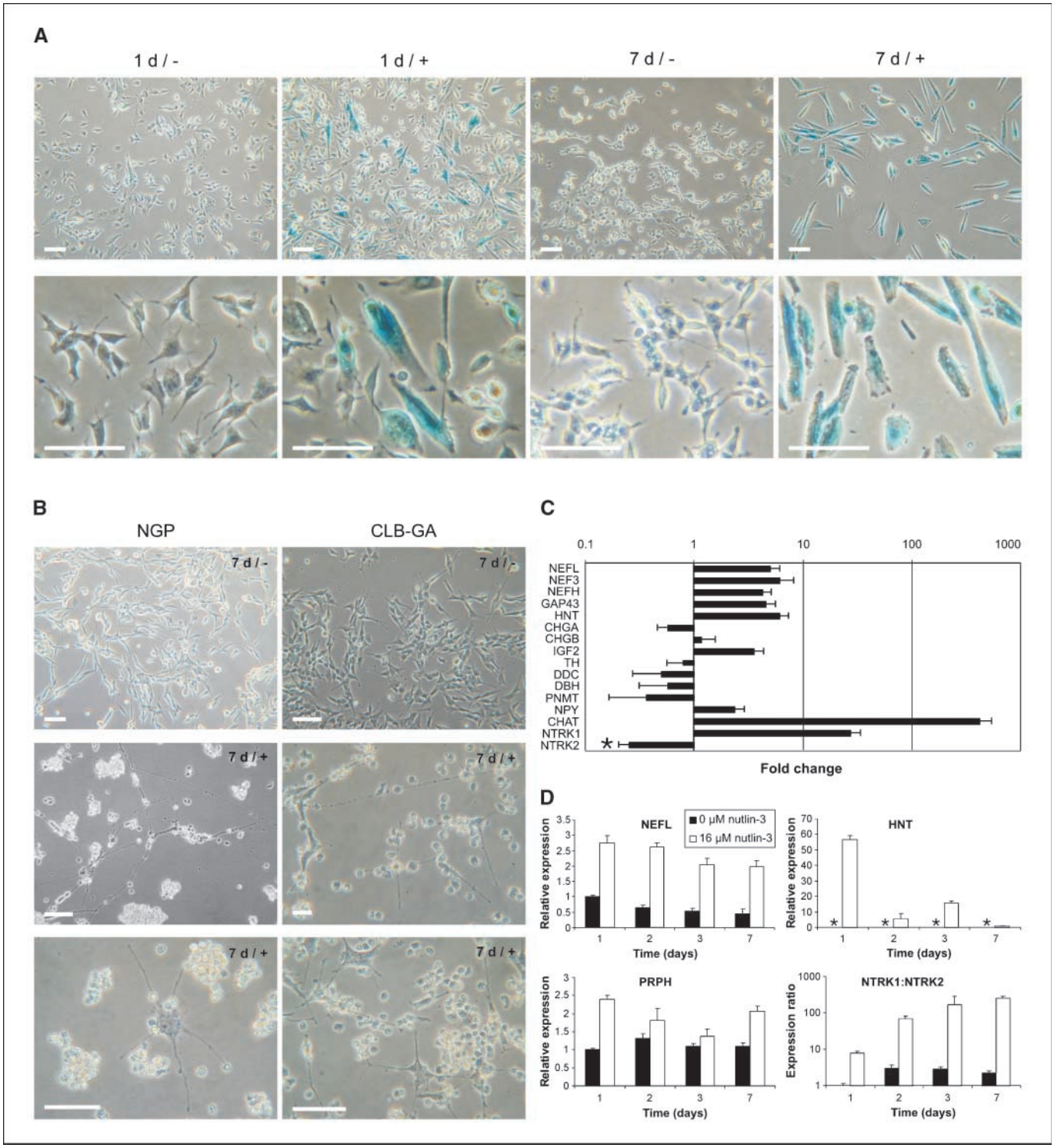

Figure 4. Induction of premature cellular senescence in surviving SK-N-SH cells and sympathetic neuronal differentiation in surviving NGP and CLB-GA cells by nutlin-3. *A,* cellular morphology and SA-β-gal staining of SK-N-SH cells treated with vehicle control (−) or 16 μmol/L nutlin-3 (+) for 1 day (*left*) or 7 days (*right*). Cells surviving incubation with nutlin-3 entered a state of premature cellular senescence as evidenced by their increased volume, flattened morphology, enhanced cytoplasmic granularity, and augmented SA-β-gal activity. Bar, 50 μm. *B,* phase-contrast images of NGP (*left*) and CLB-GA (*right*) cells under control conditions (−) and after treatment with 16 μmol/L nutlin-3 (+) for 7 days. Both NGP and CLB-GA cells surviving exposure to nutlin-3 displayed signs of neuronal differentiation, including a polar morphology and long neuritic processes, which formed a netlike arrangement. Bar, 50 μm. *C,* fold change of mRNA expression in NGP cells treated with 16 μmol/L nutlin-3 for 7 days relative to vehicle-treated cells for the neuronal/neuroendocrine differentiation marker genes *NEFL, NEF3, NEFH, GAP43, HNT, CHGA, CHGB, IGF2, TH, DDC, DBH, PNMT, NPY, CHAT, NTRK1*, and *NTRK2. Asterisk, NTRK2* expression no longer detectable after 16 μmol/L nutlin-3 for 7 days due to profound down-regulation; minimal fold change of *NTRK2* expression is displayed. *Columns,* mean of two different RT-PCR analyses; *bars,* SE. *D,* relative mRNA expression levels of *NEFL, HNT*, and *PRPH* and mRNA expression ratio of *NTRK1* to *NTRK2* in CLB-GA cells after exposure to 0 or 16 μmol/L nutlin-3 for 1, 2, 3, or 7 days. *Asterisk, HNT* expression not detectable in vehicle-treated CLB-GA cells. *Columns,* mean of two different RT-PCR measurements; *bars,* SE. Relative mRNA expression levels of the complete set of neuronal/neuroendocrine differentiation marker genes studied are available as Supplementary Data, Figs. S4 (NGP) and S5 (CLB-GA).

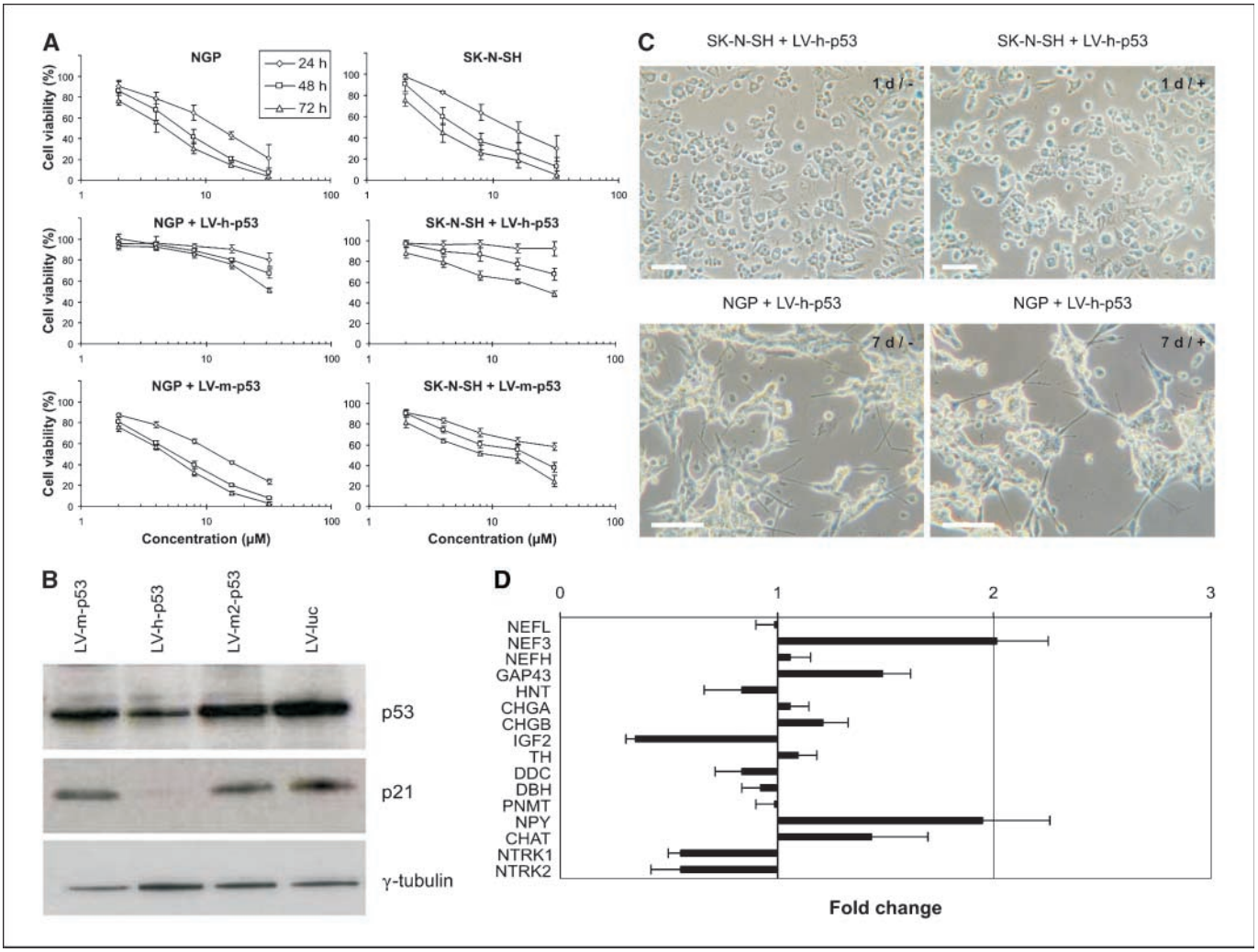

Figure 5. Induction of premature senescence in SK-N-SH cells and neuronal differentiation in NGP cells by nutlin-3 is p53 dependent. *A,* effect of nutlin-3 on cell viability of uninfected cells (*top*), cells infected with a lentiviral vector carrying a shRNA construct against human p53 (LV-h-p53; *middle*), and cells infected with a control lentiviral vector encoding a shRNA specific for murine p53 (LV-m-p53; *bottom*) for cell lines NGP and SK-N-SH. Results are percentage cell viability with respect to vehicle control-treated cells. *Points,* average of three different experiments, each done in duplicate; *bars,* SD. *B,* Western blot analysis of p53 and $p21^{WAF1/CIP1}$ expression after treatment with 16 μmol/L nutlin-3 for 24 hours in SK-N-SH cells infected with LV-m-p53, LV-h-p53, and two additional control shRNA lentiviral vectors targeting a different region of the murine *Trp53* gene (LV-m2-p53) and firefly luciferase (LV-luc), showing selective impairment of p53 function in LV-h-p53-infected cells. Expression of γ-tubulin as a loading control. *C,* SA-β-gal staining of SK-N-SH cells infected with LV-h-p53 after treatment with 0 μmol/L (−) or 16 μmol/L nutlin-3 (+) for 1 day (*top*) and cellular morphology of NGP cells infected with LV-h-p53 after exposure to 0 μmol/L (−) or 16 μmol/L nutlin-3 (+) for 7 days (*bottom*). No differences were observed between the 0 and 16 μmol/L treated cells. Bar, 50 μm. *D,* fold change of mRNA expression in NGP cells infected with LV-h-p53 after treatment with 16 μmol/L nutlin-3 for 7 days relative to vehicle-treated cells for 7 days for the same panel of neuronal/neuroendocrine differentiation marker genes as reported in Fig. 4*C* (please mind the different scale). *Columns,* mean of two different RT-PCR analyses; *bars,* SE.

and CLB-GA cells), which depend on functional p53, as shown by abrogation of these responses when p53 is silenced using a lentiviral vector expressing shRNA. These findings reveal pleiotropic activities of nutlins to incapacitate neuroblastoma cells and make this class of compounds particularly attractive for treatment of tumors that are arrested in their differentiation as is the case in neuroblastoma.

Functional outcome of nutlin-3 treatment was primarily dependent on the mutational status of *TP53*. Nutlin-3 activity was observed in all neuroblastoma cell lines with wild-type p53 regardless of *MDM2* and *MYCN* amplification status. The absence of correlation between *MYCN* amplification status and responsiveness to nutlin-3 might suggest that MDM2 deregulation is not the critical oncogenic switch by which *MYCN*-amplified neuroblastomas acquire a more aggressive behavior than *MYCN* single copy tumors, in contrast to what has been recently proposed (32), and indicates that both neuroblastoma patients with and without *MYCN* amplification could benefit from treatment with MDM2 antagonists. Several additional genomic aberrations are commonly found in neuroblastoma, including loss of 1p, 3p, and 11q and gain of 17q, enabling classification of neuroblastoma patients into different clinicogenetic subgroups (33). Genomic copy number alterations for the panel of neuroblastoma cell lines in this study will be published elsewhere.[7] For none of the frequently altered

[7] E. Michels, J. Vandesompele, K. De Preter, J. Vermeulen, A. Schramm, J. Hoebeeck, B. Menten, B. Marques, R. Stallings, V. Combaret, C. Devalck, A. De Paepe, A. Eggert, G. Laureys, N. Van Roy, and F. Speleman. ArrayCGH profiling of neuroblastoma: new insights and challenges in genomic subtype classification, in preparation.

genomic regions in neuroblastoma could a significant association with nutlin-3 responsiveness be shown, although it is possible that additional genetic defects may exist that attenuate or modify the response to nutlin-3.

Of note is that SK-N-BE(2c) and SK-N-FI cells with *TP53* mutation consistently displayed some degree of cell viability reduction when exposed to high nutlin-3 concentrations. This might theoretically reflect general cytotoxicity of nutlin compounds, residual activity of p53 missense mutants, or p53-independent activities of nutlin-3 and is thus an issue that needs to be addressed more closely to uncover whether this might curtail or favor therapeutic usefulness. One possible explanation concerns the p53 homologues p63 and p73, which are also able to suppress cell growth and induce apoptosis. Physical interaction between p73 and MDM2 resulting in inhibition of p73 transactivating activity has been clearly established (34, 35), whereas for p63 conflicting results on the relationship with MDM2 exist (36–40). Interestingly, the ability of p53 to bind MDM2 is primarily dependent on a triad of hydrophobic amino acids (F19-W23-L26), which insert deeply into a hydrophobic cleft on the surface of MDM2 (41), and this FWL motif is evolutionary conserved among p53, p63, and p73 despite a high degree of degeneration of the surrounding region. Activity of nutlin compounds relies on their structural mimicry to the conformation of the FWL motif (8). Thus, the conserved FWL motif in p63 and p73 might act as a binding site for MDM2, and nutlins might in turn disrupt the interaction between MDM2 and p53 family members, which could result in the observed increase in caspase-3 and caspase-7 activity in SK-N-BE(2c) cells after treatment with 32 μmol/L nutlin-3 for 12 and 24 hours.

From a clinical perspective, the observation of premature senescence and neuronal differentiation as treatment effects parallel to G_1 arrest and apoptosis is of substantial interest. Contribution of cellular senescence and differentiation to treatment outcome *in vivo* has been shown for conventional chemotherapy (26, 42). Our results suggest that a similar situation may be applicable to targeted therapeutics and indicate the feasibility of exploiting, by a single targeted intervention, the multitude of anticancer activities carried out by major tumor suppressors as p53. In addition, addressing multiple cellular programs could provide important failsafe mechanisms countering attempts of cancer cells to escape from therapy.

The differentiation process elicited by nutlin-3 in NGP and CLB-GA cells was characterized by expression analysis of well-established sympathetic neuronal or neuroendocrine marker genes. Neuroblastoma cells are arrested at immature stages of sympathetic differentiation, impairing the normal development into neuronal/ganglionic and neuroendocrine chromaffin cell lineages. The extensive neurite outgrowth, the expression of *NEFL, NEF3, NEFH, HNT*, and *GAP43*, the decrease in *CHGA* expression, and the neurotransmitter profile (*NPY* and *CHAT*) strongly suggest that the surviving fraction of nutlin-3-treated NGP cells matures along a sympathetic cholinergic neuronal lineage, a phenomenon also reported on retinoic acid treatment of cultured neuroblastoma cells (43, 44). In CLB-GA cells, nutlin-3 promoted a noncholinergic sympathetic neuronal differentiation, with an initial transient coexpression of sympathetic neuronal and neuroendocrine markers reminiscent of the mixed neuronal/neuroendocrine phenotype in some maturing neuroblastoma tumors (27). Furthermore, both nutlin-3-treated NGP and CLB-GA cells acquired a >100-fold shift in the neurotrophin receptor expression profile toward a higher *NTRK1* to *NTRK2* ratio, indicative of a less aggressive phenotype.

In summary, our data show that targeted disruption of the p53-MDM2 interaction unchains the powerful antitumor capacities of p53 in neuroblastoma cells by inducing a unique combination of G_1 arrest, apoptosis, premature senescence, and neuronal differentiation. If confirmed *in vivo*, selective MDM2 antagonists could offer a novel therapy concept for treatment of neuroblastoma patients with and without *MYCN* amplification by inducing tumor growth inhibition, regression, and maturation.

Acknowledgments

Received 3/1/2006; revised 7/11/2006; accepted 8/8/2006.

Grant support: The Fund for Scientific Research-Flanders (FWO) grants 011F4004 (T. Van Maerken, research assistant), G.1.5.243.05 (J. Vandesompele, postdoctoral researcher), and G.0185.04; GOA grant 12051203; Belgian Kids' Foundation grant (J. Vermeulen); Belgian Foundation against Cancer grant (S. De Clercq); Ghent Childhood Cancer Fund grant; and a VIB PhD fellowship (I. Lambertz).

The costs of publication of this article were defrayed in part by the payment of page charges. This article must therefore be hereby marked *advertisement* in accordance with 18 U.S.C. Section 1734 solely to indicate this fact.

We thank J. Lunec (Cancer Research Unit, The Medical School, University of Newcastle, Newcastle, United Kingdom) for providing the SK-N-BE(2c) cells, V. Combaret (Institut National de la Santé et de la Recherche Médicale U590, Centre Léon Bérard, Université Claude Bernard Lyon, Lyon, France) for CLB-GA cells, R. Versteeg (Department of Human Genetics, Academic Medical Center, University of Amsterdam, Amsterdam, the Netherlands) for the other neuroblastoma cells, P. Degrave and G. De Vos for cell cultures, F. Pattyn for advice, and S. Van Belle for support of this work.

References

1. Vousden KH, Lu X. Live or let die: the cell's response to p53. Nat Rev Cancer 2002;2:594–604.
2. Olivier M, Eeles R, Hollstein M, Khan MA, Harris CC, Hainaut P. The IARC TP53 database: new online mutation analysis and recommendations to users. Hum Mutat 2002;19:607–14.
3. Momand J, Wu HH, Dasgupta G. MDM2—master regulator of the p53 tumor suppressor protein. Gene 2000;242:15–29.
4. Kohn KW, Pommier Y. Molecular interaction map of the p53 and Mdm2 logic elements, which control the Off-On switch of p53 in response to DNA damage. Biochem Biophys Res Commun 2005;331:816–27.
5. Barak Y, Juven T, Haffner R, Oren M. mdm2 expression is induced by wild type p53 activity. EMBO J 1993;12:461–8.
6. Wu X, Bayle JH, Olson D, Levine AJ. The p53-mdm-2 autoregulatory feedback loop. Genes Dev 1993;7:1126–32.
7. Momand J, Jung D, Wilczynski S, Niland J. The MDM2 gene amplification database. Nucleic Acids Res 1998;26:3453–9.
8. Vassilev LT, Vu BT, Graves B, et al. *In vivo* activation of the p53 pathway by small-molecule antagonists of MDM2. Science 2004;303:844–8.
9. Vassilev LT. Small-molecule antagonists of p53-MDM2 binding: research tools and potential therapeutics. Cell Cycle 2004;3:419–21.
10. Kojima K, Konopleva M, Samudio IJ, et al. MDM2 antagonists induce p53-dependent apoptosis in AML: implications for leukemia therapy. Blood 2005;106:3150–9.
11. Stuhmer T, Chatterjee M, Hildebrandt M, et al. Nongenotoxic activation of the p53 pathway as a therapeutic strategy for multiple myeloma. Blood 2005;106:3609–17.
12. Tweddle DA, Pearson AD, Haber M, et al. The p53 pathway and its inactivation in neuroblastoma. Cancer Lett 2003;197:93–8.
13. Rodriguez-Lopez AM, Xenaki D, Eden TO, Hickman JA, Chresta CM. MDM2 mediated nuclear exclusion of p53 attenuates etoposide-induced apoptosis in neuroblastoma cells. Mol Pharmacol 2001;59:135–43.
14. Corvi R, Savelyeva L, Amler L, Handgretinger R, Schwab M. Cytogenetic evolution of MYCN and MDM2 amplification in the neuroblastoma LS tumour and its cell line. Eur J Cancer 1995;31A:520–3.
15. Corvi R, Savelyeva L, Breit S, et al. Non-syntenic amplification of MDM2 and MYCN in human neuroblastoma. Oncogene 1995;10:1081–6.
16. Van Roy N, Forus A, Myklebost O, Cheng NC, Versteeg R, Speleman F. Identification of two distinct chromosome 12-derived amplification units in neuroblastoma cell line NGP. Cancer Genet Cytogenet 1995;82:151–4.
17. Carr J, Bell E, Pearson AD, et al. Increased frequency of aberrations in the p53/MDM2/p14ARF pathway in neuroblastoma cell lines established at relapse. Cancer Res 2006;66:2138–45.

18. Thompson PM, Maris JM, Hogarty MD, et al. Homozygous deletion of CDKN2A (p16INK4a/p14ARF) but not within 1p36 or at other tumor suppressor loci in neuroblastoma. Cancer Res 2001;61:679–86.

19. Slack A, Chen Z, Tonelli R, et al. The p53 regulatory gene MDM2 is a direct transcriptional target of MYCN in neuroblastoma. Proc Natl Acad Sci U S A 2005;102:731–6.

20. Lu W, Pochampally R, Chen L, Traidej M, Wang Y, Chen J. Nuclear exclusion of p53 in a subset of tumors requires MDM2 function. Oncogene 2000;19:232–40.

21. De Preter K, Speleman F, Combaret V, et al. Quantification of MYCN, DDX1, and NAG gene copy number in neuroblastoma using a real-time quantitative PCR assay. Mod Pathol 2002;15:159–66.

22. Pattyn F, Robbrecht P, De Paepe A, Speleman F, Vandesompele J. RTPrimerDB: the real-time PCR primer and probe database, major update 2006. Nucleic Acids Res 2006;34:D684–8.

23. Vandesompele J, De Paepe A, Speleman F. Elimination of primer-dimer artifacts and genomic coamplification using a two-step SYBR green I real-time RT-PCR. Anal Biochem 2002;303:95–8.

24. Vandesompele J, De Preter K, Pattyn F, et al. Accurate normalization of real-time quantitative RT-PCR data by geometric averaging of multiple internal control genes. Genome Biol 2002;3:RESEARCH0034.

25. Tweddle DA, Malcolm AJ, Bown N, Pearson AD, Lunec J. Evidence for the development of p53 mutations after cytotoxic therapy in a neuroblastoma cell line. Cancer Res 2001;61:8–13.

26. Schmitt CA, Fridman JS, Yang M, et al. A senescence program controlled by p53 and p16INK4a contributes to the outcome of cancer therapy. Cell 2002;109:335–46.

27. Gestblom C, Hoehner JC, Hedborg F, Sandstedt B, Pahlman S. *In vivo* spontaneous neuronal to neuroendocrine lineage conversion in a subset of neuroblastomas. Am J Pathol 1997;150:107–17.

28. Hoehner JC, Gestblom C, Hedborg F, Sandstedt B, Olsen L, Pahlman S. A developmental model of neuroblastoma: differentiating stroma-poor tumors' progress along an extra-adrenal chromaffin lineage. Lab Invest 1996;75:659–75.

29. Pahlman S, Hoehner JC, Nanberg E, et al. Differentiation and survival influences of growth factors in human neuroblastoma. Eur J Cancer 1995;31:A453–8.

30. Schramm A, Schulte JH, Astrahantseff K, et al. Biological effects of TrkA and TrkB receptor signaling in neuroblastoma. Cancer Lett 2005;228:143–53.

31. Maris JM, Matthay KK. Molecular biology of neuroblastoma. J Clin Oncol 1999;17:2264–79.

32. Slack A, Shohet JM. MDM2 as a critical effector of the MYCN oncogene in tumorigenesis. Cell Cycle 2005;4:857–60.

33. Vandesompele J, Baudis M, De Preter K, et al. Unequivocal delineation of clinicogenetic subgroups and development of a new model for improved outcome prediction in neuroblastoma. J Clin Oncol 2005;23:2280–99.

34. Balint E, Bates S, Vousden KH. Mdm2 binds p73α without targeting degradation. Oncogene 1999;18:3923–9.

35. Zeng X, Chen L, Jost CA, et al. MDM2 suppresses p73 function without promoting p73 degradation. Mol Cell Biol 1999;19:3257–66.

36. Kojima T, Ikawa Y, Katoh I. Analysis of molecular interactions of the p53-family p51(p63) gene products in a yeast two-hybrid system: homotypic and heterotypic interactions and association with p53-regulatory factors. Biochem Biophys Res Commun 2001;281:1170–5.

37. Little NA, Jochemsen AG. Hdmx and Mdm2 can repress transcription activation by p53 but not by p63. Oncogene 2001;20:4576–80.

38. Wang X, Arooz T, Siu WY, et al. MDM2 and MDMX can interact differently with ARF and members of the p53 family. FEBS Lett 2001;490:202–8.

39. Okada Y, Osada M, Kurata S, et al. p53 gene family p51(p63)-encoded, secondary transactivator p51B(TAp63α) occurs without forming an immunoprecipitable complex with MDM2, but responds to genotoxic stress by accumulation. Exp Cell Res 2002;276:194–200.

40. Calabro V, Mansueto G, Parisi T, Vivo M, Calogero RA, La Mantia G. The human MDM2 oncoprotein increases the transcriptional activity and the protein level of the p53 homolog p63. J Biol Chem 2002;277:2674–81.

41. Kussie PH, Gorina S, Marechal V, et al. Structure of the MDM2 oncoprotein bound to the p53 tumor suppressor transactivation domain. Science 1996;274:948–53.

42. Raza A, Preisler H, Lampkin B, et al. Clinical and prognostic significance of *in vivo* differentiation in acute myeloid leukemia. Am J Hematol 1993;42:147–57.

43. Sidell N, Lucas CA, Kreutzberg GW. Regulation of acetylcholinesterase activity by retinoic acid in a human neuroblastoma cell line. Exp Cell Res 1984;155:305–9.

44. Edsjo A, Lavenius E, Nilsson H, et al. Expression of trkB in human neuroblastoma in relation to MYCN expression and retinoic acid treatment. Lab Invest 2003;83:813–23.